Publication IV

H. Mäki and R. J. Ilmoniemi. Projecting out muscle artifacts from TMS-evoked EEG. *NeuroImage*, 54, 2706–2710, 2011.

NeuroImage 54 (2011) 2706–2710

Contents lists available at ScienceDirect

NeuroImage

journal homepage: www.elsevier.com/locate/ynimg

Projecting out muscle artifacts from TMS-evoked EEG

Hanna Mäki *, Risto J. Ilmoniemi

Department of Biomedical Engineering and Computational Science (BECS), Aalto University, P.O. Box 12200, FI-00076 Aalto, Espoo, Finland
BioMag Laboratory, HUSLAB, Helsinki University Central Hospital, P.O. Box 340, FI-00029 HUS, Helsinki, Finland

ARTICLE INFO

Article history:
Received 18 October 2010
Accepted 10 November 2010
Available online 18 November 2010

Keywords:
Transcranial magnetic stimulation
Electroencephalography
Broca's area
Principal component analysis
Signal-space projection

ABSTRACT

Transcranial magnetic stimulation combined with electroencephalography is a powerful tool for probing cortical excitability and connectivity; we can perturb one brain area and study the reactions at the stimulated and interconnected sites. When stimulating areas near cranial muscles, their activation produces a large artifact in the electroencephalographic signal, lasting tens of milliseconds and masking the early brain signals. We present an artifact removal method based on projecting out the topographic patterns of the muscle activity. Although the brain and muscle components overlap both temporally and spectrally, the fact that muscle activity is present also at frequencies higher than 100 Hz, while brain signal is mostly restricted to frequencies lower than that, allows us to study the high-frequency muscle activity without brain contribution. We determined the muscle activity topographies from data highpass-filtered at a 100-Hz cutoff frequency using principal component analysis. Projecting out the topographies of the principal components which explain most of the variance of the high-frequency data reduces not only the high-frequency activity but also the low-frequency muscle contribution, because the topography produced by a muscle source can be expected to be the same regardless of the frequency. The method greatly reduced the muscle artifact evoked by stimulation of Broca's area, while a significant brain signal contribution remained. Improvement in the signal-to-artifact ratio, defined as the relative amplitudes of brain signals peaking after 50 ms and the first artifact deflection, was of the order of 10–100 depending on the number of projections. The presented artifact removal method enables one to study the cortical state when stimulating areas near the cranial muscles.

Introduction

Transcranial magnetic stimulation (TMS) can be used to activate the brain in a controlled and direct manner (Barker et al., 1985). Combined with electroencephalography (EEG), TMS is a powerful tool for probing the cortical state (Ilmoniemi et al., 1997). TMS–EEG has been successfully applied to study cortical excitability and connectivity during stimulation of, e.g., the primary motor cortex (M1; see, e.g., Komssi et al., 2002), premotor areas (Massimini et al., 2005), prefrontal cortex (Daskalakis et al., 2008; Fitzgerald et al., 2009; Kähkönen et al., 2004, 2005), primary somatosensory cortex (Raij et al., 2008), as well as parietal and associative visual areas (Rosanova et al., 2009). These sites are relatively far away from the cranial muscles and hence, for most subjects, stimulation of these areas does not produce marked muscle artifacts. On the contrary, especially the stimulation of the lateral sites activates cranial muscles and produces muscle artifacts, which can be a few orders of magnitude larger than the brain signal and last tens of milliseconds. In addition, facial muscles may be activated through stimulation of trigeminal nerve fibers. The muscle artifacts mask the early EEG deflections, which are of great interest in terms of cortical excitability and connectivity.

We present a method to remove the large muscle artifacts from TMS-evoked EEG signals and apply it on data recorded following the stimulation of Broca's area. When a muscle is active, the currents produce certain topographies, i.e., spatial signal patterns detected on the scalp. In other words, a topography can be defined as the time-invariant relative signal amplitudes measured by each channel as a result of a given current source. If the topographies are known, they can be removed using signal-space projection (SSP; Uusitalo and Ilmoniemi, 1997). Each projection reduces the dimension of the EEG signal by one, removing all signal components parallel to the given topography and preserving the signal components orthogonal to it. The problem in determining the topographies is that the early TMS-evoked brain activity coincides temporally with the artifact. These signals overlap also spectrally, but muscle activity is generally present also at higher frequencies than brain activity. The EEG signal originating from the brain is typically restricted to frequencies below 100 Hz because of the relatively slow synchronous postsynaptic activity and the difficulty in detecting high-frequency action potentials with EEG mostly because of their behavior as current quadrupoles, the electric field of which falls off rapidly as a function of distance (r^{-3}; Plonsey,

* Corresponding author. Department of Biomedical Engineering and Computational Science (BECS), Aalto University, P.O. Box 12200, FI-00076 Aalto, Espoo, Finland. Fax: +358 9 470 23182.
E-mail addresses: hanna.maki@tkk.fi (H. Mäki), risto.ilmoniemi@tkk.fi (R.J. Ilmoniemi).

1053-8119/$ – see front matter © 2010 Elsevier Inc. All rights reserved.
doi:10.1016/j.neuroimage.2010.11.041

1977), and because of lack of synchrony. In contrast, muscle activity is normally manifested also at higher frequencies (below 400–500 Hz) in the surface electromyographic (EMG) signal (Clancy et al., 2002; Merletti, 1996), reflecting the summed motor unit action potentials. Since the spectra of brain and muscle activity overlap at frequencies below 100 Hz, lowpass-filtering is not adequate to remove the artifacts. On the contrary, highpass-filtering the signal with a cutoff frequency around 100 Hz results in data containing mainly muscle activity and noise. Assuming that the low-frequency components of the muscle activity originate in the same muscles as the high-frequency components, they can be expected to be composed of similar current distributions and thus to have similar topographies. As a result, projecting out the topographies of the high-frequency muscle activity would also remove the contribution of the low-frequency muscle activity, which overlaps spectrally with the brain activity.

Methods

Theory of the artifact removal method

The TMS-evoked d-dimensional EEG signal (measured with $d+1$ electrodes) is a weighted sum of signals originating from the brain and muscles as well as noise. Both brain and muscle signals can be further divided into high- and low-frequency components according to a frequency threshold f_{th}. Let $\boldsymbol{x}_i$ and $\boldsymbol{y}_i$ represent the d-dimensional time-independent signal-space vectors, i.e., topographies, of muscle and brain activity sources, respectively, describing the relative signal amplitudes measured with the electrodes as a result of respective source activation. Let $a_i(t)$ and $b_i(t)$ be the time-varying amplitudes of the muscle artifact and brain sources, respectively. Thus, a signal $\boldsymbol{m}(t)$ can be described as a sum of N^{L} low-frequency and N^{H} high-frequency muscle artifact components as well as M^{L} low-frequency and M^{H} high-frequency brain components and noise $\boldsymbol{n}(t)$:

$$\boldsymbol{m}(t) = \sum_{i=1}^{N^{\mathrm{L}}} a_i^{\mathrm{L}}(t)\boldsymbol{x}_i^{\mathrm{L}} + \sum_{i=1}^{N^{\mathrm{H}}} a_i^{\mathrm{H}}(t)\boldsymbol{x}_i^{\mathrm{H}} + \sum_{i=1}^{M^{\mathrm{L}}} b_i^{\mathrm{L}}(t)\boldsymbol{y}_i^{\mathrm{L}} + \sum_{i=1}^{M^{\mathrm{H}}} b_i^{\mathrm{H}}(t)\boldsymbol{y}_i^{\mathrm{H}} + \boldsymbol{n}(t), \quad (1)$$

where the superscripts L and H refer to low- and high-frequency components. When f_{th} is chosen so that the proportion of high-frequency EEG signal originating from the brain is negligible $\left(\sum_{i=1}^{M^{\mathrm{H}}} b_i^{\mathrm{H}}(t)\boldsymbol{y}_i^{\mathrm{H}} \approx 0\right)$, highpass-filtering the signal with a cutoff frequency f_{th} results in a signal that consists mainly of the high-frequency components of the muscle activity and noise:

$$\mathrm{H}(\boldsymbol{m}(t)) \approx \sum_{i=1}^{N^{\mathrm{H}}} a_i^{\mathrm{H}}(t)\boldsymbol{x}_i^{\mathrm{H}} + \mathrm{H}(\boldsymbol{n}(t)), \quad (2)$$

where H is the highpass-filter operator. If the low-frequency muscle components belong to the signal subspace spanned by the high-frequency muscle components $\left(\left\{\boldsymbol{x}_1^{\mathrm{L}}, \ldots \boldsymbol{x}_{N_{\mathrm{L}}}^{\mathrm{L}}\right\} \in \mathrm{span}\left(\boldsymbol{x}_1^{\mathrm{H}}, \ldots \boldsymbol{x}_{N_{\mathrm{H}}}^{\mathrm{H}}\right)\right)$, projecting out the topographies of the highpass-filtered data also removes the low-frequency muscle components.

Principal component analysis (PCA; Pearson, 1901) can be used to transform the highpass-filtered data to orthonormal eigenvectors $\boldsymbol{\mu}_j$, i.e., the high-frequency principal component (PC) topographies, each being a linear combination of the original variables (EEG signals) and associated with respective eigenvalues s_j and time-varying amplitudes $\alpha_j(t)$:

$$\mathrm{H}(\boldsymbol{m}(t)) = \sum_{j=1}^{d} \alpha_j(t)\boldsymbol{\mu}_j. \quad (3)$$

Since noise is present in all signal-space directions, the highpass-filtered data consist of d orthogonal components. Therefore, projecting out all the dimensions of the highpass-filtered data from the original signal would remove all data. The PCs with the largest eigenvalues reflect the largest amount of variance in the data and thus the muscle artifacts at least in cases where they are much larger than the noise. Accordingly, projecting out N PCs ($N<d$), i.e., high-frequency topographies, with the largest eigenvalues using SSP (Uusitalo and Ilmoniemi, 1997) reduces the muscle artifact:

$$\boldsymbol{m}_{\mathrm{corr}}(t) = \boldsymbol{m}(t) - \sum_{j=1}^{N} \boldsymbol{\mu}_j\boldsymbol{\mu}_j^{\mathrm{T}}\boldsymbol{m}(t), \quad (4)$$

where the PCs $\boldsymbol{\mu}_j$ have been sorted according to the corresponding eigenvalues in decreasing order ($s_1 \geq s_2 \geq \ldots \geq s_N$), $\boldsymbol{m}_{\mathrm{corr}}(t)$ is the corrected signal, and T stands for transpose.

Experimental methods

The study was approved by the Ethics Committee of the Helsinki University Central Hospital and was performed in compliance with the Declaration of Helsinki. Broca's area of one male (S1, 22 years old), and two females (S2, 23; S3, 27), who gave their written informed consent before the experiment, was stimulated with Nexstim eXimia TMS stimulator (Nexstim Ltd., Helsinki, Finland) and its figure-of-8 biphasic coil (average coil winding diameter 50 mm). Nexstim eXimia navigated brain stimulation system (NBS) was used to target the stimulation to the lateral end of the precentral sulcus, with the maximal induced current directed anteriorly, towards the inferior frontal gyrus. 160 (S1 and S2) or 120 (S3) pulses were delivered with a stimulation intensity adjusted to produce a stimulation effect similar to that when the M1 hand area was stimulated at 100% of the resting motor threshold (MT; 5/10 motor evoked potentials >50 μV) determined from the abductor pollicis brevis (APB) with Nexstim eXimia EMG system; the electric field on the cortical surface as calculated by the NBS software during the stimulation of Broca's area was the same as during M1 stimulation with the intensity 100% of MT (130 V/m (S1), 108 V/m (S2), or 120 V/m (S3)). EEG was recorded with the TMS-compatible 60-channel Nexstim eXimia EEG system. The reference and ground electrodes were placed behind the right ear and on the right cheek bone, respectively. Electrooculogram (EOG) electrodes were placed above the right eye and on the left side of the left eye. The signals were bandpass-filtered at 0.1–350 Hz and digitized at 1450 Hz. The impedances were kept below 5 kΩ. Subjects S1 and S3 listened to masking white noise during the stimulation, which markedly attenuated the perception of the coil click. Subject S2 only wore earplugs, because TMS disturbed the functioning of the earphones in that experiment.

Data analysis

Data analysis was performed with MATLAB (The Mathworks, Inc., Natick, Massachusetts, USA). Based on visual inspection of the signals, data from one disconnected electrode (C4 (S1) or CP2 (S2 and S3)) and epochs with eye movements as determined from the EOG signals were rejected. The raw data were highpass-filtered with a 2nd-order Butterworth filter and a cutoff frequency of 100 Hz (roll-off 40 dB/dec). The high-frequency data were averaged over accepted epochs at 0–30 ms with respect to the stimuli, and the PCs of the averaged data were determined with PCA. SSP was applied to project out the signal components belonging to the subspace spanned by the EEG topographies that correspond to the high-frequency (Eq. (4)). The projections were applied to the original unfiltered data. The PCs were sorted according to their eigenvalues and projected out in that order, the component with the largest eigenvalue first. The global mean field amplitude (GMFA; Lehmann and Skrandies, 1980) reflecting the overall EEG response,

$$\mathrm{GMFA}(t) = \sqrt{\left[\sum_{k=1}^{d} \left(x_k(t) - x_k^{\mathrm{mean}}(t)\right)^2\right] \Big/ d} \quad (5)$$

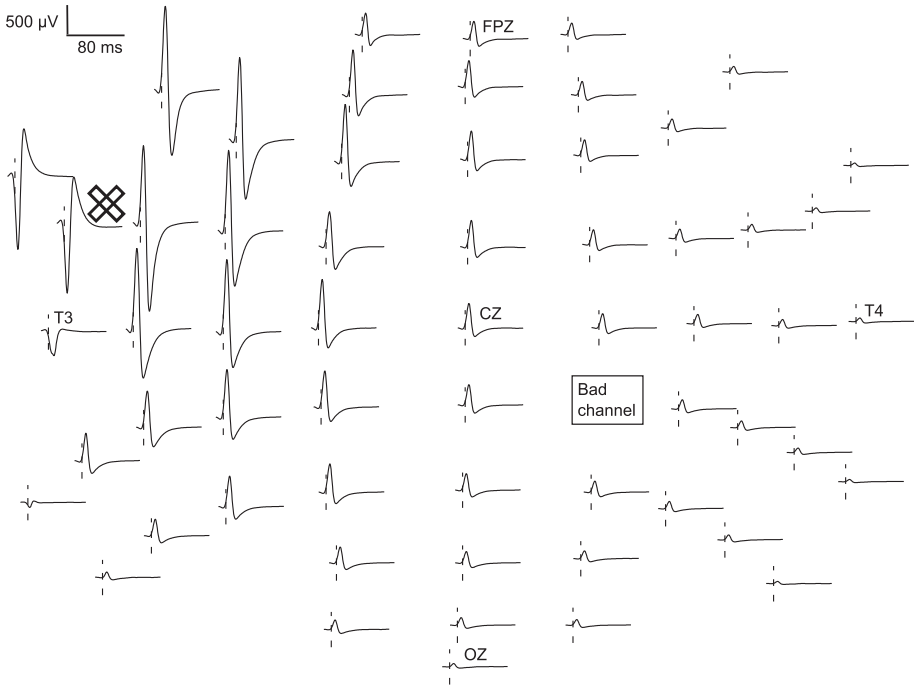

Fig. 1. Filtered (2–80 Hz) data of subject S3 before artifact removal presented in the layout of the EEG cap. The strong muscle artifact masks the early brain responses. Because of the voltage scale, no details of the later brain signals are visible. The names of some electrodes according to the 10–20 system have been marked. The cross marks the stimulation site.

where $x_k(t)$ is the signal of channel k highpass-filtered with a 1st-order Butterworth filter and a cutoff frequency of 2 Hz to remove slow drifts and $x_k^{\mathrm{mean}}(t) = d^{-1}\sum_{k=1}^{d} x_k(t)$ is the mean signal over the channels, was calculated from the original data and after projecting out each component; the amplitudes and latencies of the GMFA peaks were determined manually. The signal-to-artifact ratios, defined as the amplitude of each GMFA peak appearing later than 50 ms after the stimulus divided by the amplitude of the first GMFA peak assumed to reflect the muscle artifact, were determined as well. 95% confidence intervals of the GMFAs obtained after the projections were determined with one-sample *t*-tests. A Bonferroni correction for multiple comparisons was applied on the confidence intervals; since the number of brain response deflections identified in the original GMFAs was 5, it was used as the number of comparisons in the corrections. A GMFA peak was considered statistically significant if its confidence interval did not overlap with that of the baseline (−50…0 ms). For visualization purposes, both the original and the corrected data were bandpass-filtered with a 2nd-order Butterworth filter (2–80 Hz) and averaged over epochs.

Results

The stimulation of Broca's area produced a biphasic muscle artifact (Fig. 1), the first deflection peaking at 5 ± 1 ms (mean ± sd over subjects) and the second at 10 ± 2 ms as determined from the GMFA. The second component decayed slowly and returned to the baseline level at around 40–50 ms. In addition to the artifact deflections, which were named A1 and A2, the GMFA of the original data was composed of four deflections peaking at 84 ± 7, 141 ± 28, 195 ± 20, and 280 ± 5 ms (named B2–B5 in the order of the latencies). In the original GMFA of subject S1, there was another peak at 54 ms (B1), which appeared in the GMFAs of subjects S2 (62 ms) and S3 (56 ms) after projecting out the first PC (see Fig. 2 for the topographies of the 3 PCs with the largest eigenvalues). The GMFAs of all the subjects, after projecting out 30 PCs, are presented in Fig. 3. The seven peaks (A1–A2, B1–B5) were identified in the GMFAs of all the subjects after each projection step. After 30

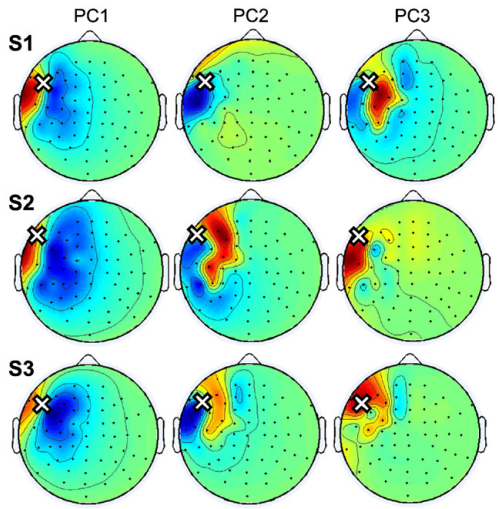

Fig. 2. Topographies of the three PCs with the largest eigenvalues of all subjects S1–S3. The white cross marks the stimulation site. The first PC is remarkably similar in all the subjects.

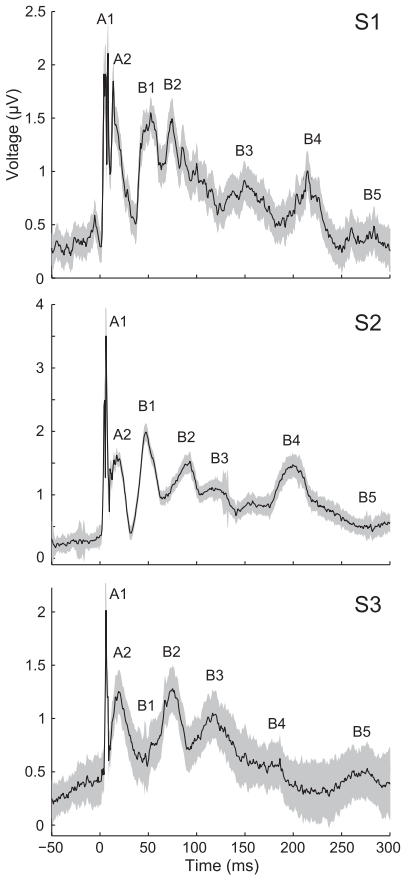

Fig. 3. GMFAs of all the subjects S1–S3 calculated after projecting out 30 PCs (see Fig. 2 for the first 3 PCs) according to Eq. (4). As a result of the projections, the originally large muscle artifact is of the same order of magnitude as the later brain responses. The shaded area indicates the 95% confidence interval, which shows that the brain response peaks B2–B3 of all the subjects and peaks B1 and B4 of S1 and S2 are statistically significant after the projections.

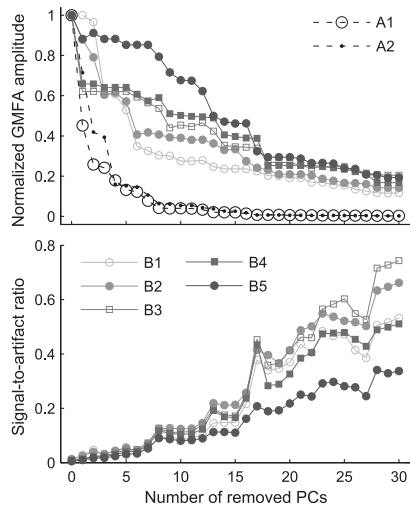

Fig. 4. The amplitude of each GMFA peak normalized with the original value (top; B1 amplitude normalized with the value after projecting out 1 PC) and the signal-to-artifact ratio of each GMFA peak (bottom) as a function of the number of PCs projected out. The signal-to-artifact ratio increased as a result of the projections. Data from subject S3.

projections, peaks B2 and B3 of all the subjects were statistically significant and peaks B1 and B4 were significant in the GMFAs of subjects S1 and S2, while B5 was not significant in any subject. The amplitudes of the GMFA peaks normalized with the value in the original data after projecting out 0–30 PCs and the respective signal-to-artifact ratios of subject S3 are presented in Fig. 4. The data of the other subjects showed similar results. The overall signal-to-artifact ratio, defined as the average signal amplitude of peaks B2–B5 divided by the amplitude of A1 was originally 0.011 ± 0.002 and increased to 0.47 ± 0.11 after projecting out 30 PCs (increase by factor 45 ± 16). The signal-to-artifact ratio increased with factor 1.7 ± 0.1 after removing 1 PC, with factor 10 after removing 12 (S1), 15 (S2), or 8 PCs (S3), and with factor 30 after removing 18 (S1), 27 (S2), or 17 PCs (S3). The corrected data of subject S3 after projecting out 30 PCs is presented in Fig. 5. The data in the channels near the stimulation site were attenuated the most, whereas signals in channels further away were better preserved.

Discussion

Projecting out the topographies of the components that explained the largest variance of the high-frequency EEG data greatly reduced the large muscle artifacts evoked by the stimulation of Broca's area. Although the amplitudes of the later (peaking after 50 ms) brain signal components were attenuated as well, the improvement in the signal-to-artifact ratio, defined as the relative amplitudes between the later signal components and the artifact, was of the order of 10–100, depending on the number of projected components. In addition, certain brain signal components were statistically significant after the projections. Accordingly, the method reduces the muscle artifact but preserves a significant amount of brain signal. As can be expected, the artifact reduction procedure attenuated mostly the signal in the channels near the stimulation site (see Fig. 5). Naturally, the brain signal sources that produce topographies belonging to the subspace spanned by the removed components are lost as well. Especially, brain sources near the stimulation site are likely to produce signals nearly parallel to the muscle artifact components in the signal space and thus a larger part of these signals is projected out as compared to signals originating further away from the stimulation site. Therefore, the signal-to-artifact ratio calculated here is an optimistic estimate if sources near the stimulation site are of interest, while signals from sources further away are better preserved. This suggests that the artifact removal method enables studying cortical connectivity by examining the signals originating in other parts of the brain than the stimulation site, which are also originally masked by the artifact. One of the advantages of the SSP method is that, since the projections applied are known, it is possible to apply source localization despite the distortion of the data, if the projections are taken into account when calculating the forward model (Uusitalo and Ilmoniemi, 1997). In addition, the presented method is data driven, i.e., no assumptions need to be made about the origin of the muscle artifact; thus, the method works equally well, for example, if the muscles are not activated directly but through nerves innervating them and the exact location of the muscle activity is not known. In conclusion, the method presented here enables probing cortical connectivity with TMS even when the stimulation evokes muscle artifacts in the EEG.

Acknowledgments

The authors would like to thank Johanna Metsomaa, Julio César Hernández Pavón, and Jukka Sarvas for technical assistance and

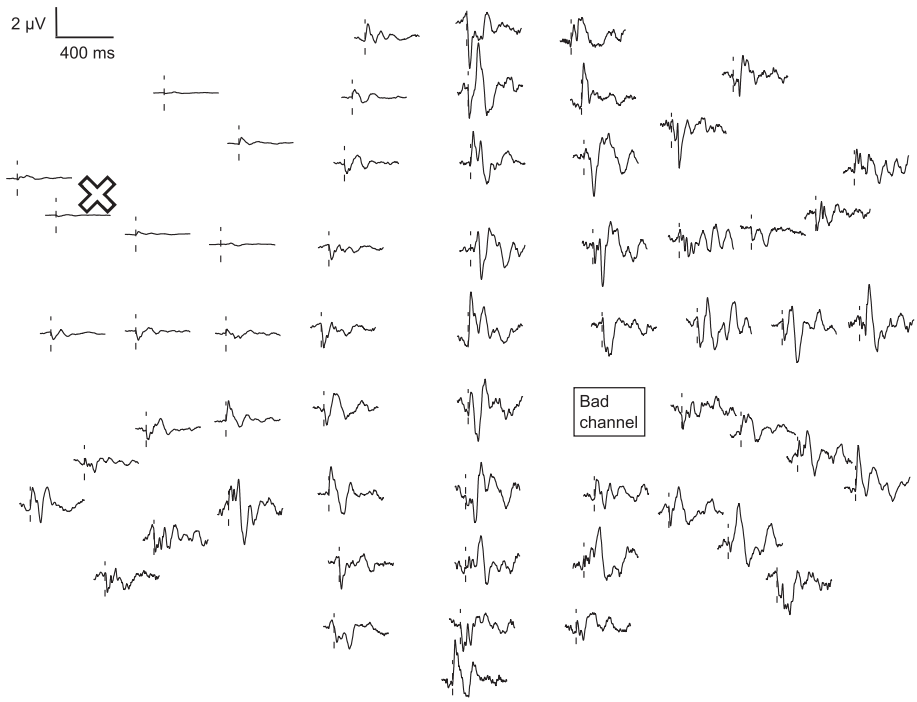

Fig. 5. Filtered (2–80 Hz) data of subject S3 after projecting out 30 PCs presented in the layout of the EEG cap. The muscle artifact is greatly reduced as a result of the projections. The signals of the channels near the stimulation site are attenuated, while further away the signals are better preserved. Even though the signals are somewhat distorted, the fact that the applied projections are known allows us to take them into account when further analyzing and interpreting the data. The cross marks the stimulation site. The nose points upwards. Note the different scale of both time and voltage axes compared to Fig. 1.

comments on the manuscript. This study was supported by the Academy of Finland (grant No: 121167 and the International Graduate School in Biomedical Engineering and Medical Physics).

References

Barker, A.T., Jalinous, R., Freeston, I.L., 1985. Non-invasive magnetic stimulation of the human motor cortex. Lancet 1, 1106–1107.
Clancy, E.A., Morin, E.L., Merletti, R., 2002. Sampling, noise-reduction and amplitude estimation issues in surface electromyography. J. Electromyogr. Kinesiol. 12, 1–16.
Daskalakis, Z.J., Farzan, F., Barr, M.S., Maller, J.J., Chen, R., Fitzgerald, P.B., 2008. Long-interval cortical inhibition from the dorsolateral prefrontal cortex: a TMS–EEG study. Neuropsychopharmacology 33, 2860–2869.
Fitzgerald, P.B., Maller, J.J., Hoy, K., Farzan, F., Daskalakis, Z.J., 2009. GABA and cortical inhibition in motor and non-motor regions using combined TMS–EEG: a time analysis. Clin. Neurophysiol. 120, 1706–1710.
Ilmoniemi, R.J., Virtanen, J., Ruohonen, J., Karhu, J., Aronen, H.J., Näätänen, R., Katila, T., 1997. Neuronal responses to magnetic stimulation reveal cortical reactivity and connectivity. NeuroReport 8, 3537–3540.
Kähkönen, S., Wilenius, J., Komssi, S., Ilmoniemi, R.J., 2004. Distinct differences in cortical reactivity of motor and prefrontal cortices to magnetic stimulation. Clin. Neurophysiol. 115, 583–588.
Kähkönen, S., Komssi, S., Wilenius, J., Ilmoniemi, R.J., 2005. Prefrontal transcranial magnetic stimulation produces intensity-dependent EEG responses in humans. Neuroimage 24, 955–960.
Komssi, S., Aronen, H.J., Huttunen, J., Kesäniemi, M., Soinne, L., Nikouline, V.V., Ollikainen, M., Roine, R.O., Karhu, J., Savolainen, S., Ilmoniemi, R.J., 2002. Ipsi- and contralateral EEG reactions to transcranial magnetic stimulation. Clin. Neurophysiol. 113, 175–184.
Lehmann, D., Skrandies, W., 1980. Reference-free identification of components of checkerboard-evoked multichannel potential fields. Electroencephalogr. Clin. Neurophysiol. 48, 609–621.
Massimini, M., Ferrarelli, F., Huber, R., Esser, S.K., Singh, H., Tononi, G., 2005. Breakdown of cortical effective connectivity during sleep. Science 309, 2228–2232.
Merletti, R., 1996. Standards for reporting EMG data. J. Electromyogr. Kinesiol. 6 (III–IV).
Pearson, K., 1901. On lines and planes of closest fit to systems of points in space. Philos. Mag. 2, 559–572.
Plonsey, R., 1977. Action potential sources and their volume conductor fields. Proc. IEEE 65, 601–611.
Raij, T., Karhu, J., Kičić, D., Lioumis, P., Julkunen, P., Lin, F.-H., Ahveninen, J., Ilmoniemi, R. J., Mäkelä, J.P., Hämäläinen, M., Rosen, B.P., Belliveau, J.W., 2008. Parallel input makes the brain run faster. Neuroimage 40, 1792–1797.
Rosanova, M., Casali, A., Bellina, V., Resta, F., Mariotti, M., Massimini, M., 2009. Natural frequencies of human corticothalamic circuits. J. Neurosci. 29, 7679–7685.
Uusitalo, M.A., Ilmoniemi, R.J., 1997. Signal-space projection method for separating MEG or EEG into components. Med. Biol. Eng. Comput. 35, 135–140.